Journal of Statistical Physics, Vol. 46, Nos. 3/4, 1987

On the Dielectric Susceptibility of Classical Coulomb Systems. II

Ph. Choquard,[1] B. Piller,[1] and R. Rentsch[1]

Received October 16, 1986

This paper deals with the shape dependence of the dielectric susceptibility (equivalently defined, in a canonical ensemble, by the mean square fluctuation of the electric polarization or by the second moment of the charge–charge correlation function) of classical Coulomb systems. The concept of partial second moment is introduced with the aim of analyzing the contributions to the total susceptibility of pairs of particles of increasing separation. For a disk-shaped one-component plasma with coupling parameter $\gamma = 2$ it is shown, numerically and algebraically for small and large systems, that (1) the correlation function of two particles close to the edge of the disk decays as the inverse of the square of their distance, and (2) the susceptibility is made up of a bulk contribution, which saturates rapidly toward the Stillinger–Lovett value, and of a surface contribution, which varies on the scale of the disk diameter and is described by a new law called the "arc sine" law. It is also shown that electrostatics and statistical mechanics with shape-dependent thermodynamic limits are consistent for the same model in a strip geometry, whereas the Stillinger–Lovett sum rule is verified for a boundary-free geometry such as the surface of a sphere. Some results of extensive computer simulations of one- and two-component plasmas in circular and elliptic geometries are shown. Anisotropy effects on the susceptibilities are clearly demonstrated and the "arc sine" law for a circular plasma is well confirmed.

KEY WORDS: One- and two-component plasmas; dielectric susceptibility; partial second moment; shape-dependent effects.

1. INTRODUCTION

This paper is a contribution to the quantitative theory of the shape dependence of the dielectric susceptibility of classical Coulomb systems.

[1] Institut de Physique Théorique, Ecole Polytechnique Fédérale de Lausanne, CH-1015 Lausanne, Switzerland.

0022-4715/87/0200-0599$05.00/0

Qualitatively, the picture is that the susceptibility is made up of two contributions: one originating from the bulk of the system, where short-range correlations dominate, and one from the surface, where long-range correlations may occur in a thin surface layer. In a previous paper,[15] referred to as I, it has already been noticed that, in order to ensure the consistency between the predictions of phenomenological electrostatics and statistical mechanics, it is essential to perform a thermodynamic limit that preserves the shape of the initially finite system. Direct calculation of the susceptibility of a two-dimensional one-component plasma (OCP) in a disk for a coupling parameter $\gamma = q^2/k_B T = 2$ produced the value $1/\pi$, which is that required by electrostatics, whereas $1/2\pi$ is the value given by the second moment Stillinger–Lovett (SL) sum rule and which corresponds to the bulk contribution. How then does the surface contribution amount exactly to $1/2\pi$ in this case? This is one of the questions to which this paper is addressed. It is organized as follows.

Section 2 recalls, for the different geometries considered in subsequent sections, the phenomenological relations between the dielectric constant of classical, homogeneously polarizable, isotropic Coulomb systems and their shape-dependent susceptibility tensor. Here this tensor is defined to relate the electric polarization density of the system confined in a certain domain and surrounded by the vacuum to the external field. Next, and in the case of spherical geometry, comments are made on the connection between the above relation, which is model independent, and the Clausius–Mossotti relation, which is model dependent and is of approximate validity. Then a heuristic argument is given to indicate that an OCP of ellipsoidal geometry has exactly the anisotropic susceptibility tensor required by the general relations in their limit of infinite dielectric constant. Lastly, it is recalled that, in a canonical ensemble, two equivalent expressions for the susceptibility tensor are available: one expression is given in terms of polarization fluctuations, hereafter called the PF formula, and the other expression is given in terms of the second moment tensor of the truncated charge–charge correlation functions, hereafter called for simplicity the second moment or SM formula. In I the PF formula only was used and the $1/\pi$ result was obtained [I, Eq. (16)], but its splitting into $1/2\pi + 1/2\pi$ could not be understood. It is for this reason that the SM formula is used here. However, since it involves the product of two Cartesian coordinates, which constitute unbounded observables, the convergence of their expectation values has to be investigated with great care. For this purpose the idea of the partial second moment is introduced.

Section 3 deals entirely with the OCP in a disk for $\gamma = 2$. In this geometry the partial second moment is isotropic and is a function of a distance that varies from zero to the disk diameter. It is shown explicitly that,

for a model with a background possessing an adequate excess charge, the pair correlation function decays as the inverse square of the distance between two points belonging to the surface layer, whereas it is Gaussian if the two points are in the interior of the disk, and that the partial second moment contains, for large systems, two additive contributions: a bulk and a surface contribution. It is found that within a very short range equal to the ion disk radius, the bulk contribution saturates toward $1/2\pi$, which is the expected SL value, whereas the surface contribution follows a new, extremely long-range "arc sine" law and reaches the value $1/2\pi$ at the disk diameter. Then the splitting of $1/\pi = 1/2\pi + 1/2\pi$ is explained in quantitative terms.

Section 4 presents exact numerical results for the OCP on a disk for $\gamma = 2$ and also some results from Monte Carlo (MC) simulations for an OCP at $\gamma = 1.5$, 2, and 4 and for a two-component plasma (TCP) at $\gamma = 2$. The "arc sine" law seems to be verified in all cases, which means that long-range correlation near a surface may be a general property of Coulomb systems. It is worth mentioning here that the theory developed in Section 3 has been greatly inspired by the Figs. 1a, 1b, and 4 in particular.

Section 5 deals with the problem of polarization fluctuations in anisotropic geometries. The MC simulations of the OCP and of a TCP for $\gamma = 2$ in three different elliptical domains are reported. The depolarization tensor of an ellipse is computed explicitly. Although the measured values of the susceptibility of the rather small systems simulated are quite smaller than the values predicted by electrostatics, their longitudinal to transverse ratios are in good agreement with the theoretical values. Expected for the OCP on the basis of the argument presented in Section 2, these results are less trivial for a TCP, since this system learns the shape of its domain only through the collisions of its particles with the walls.

Section 6 is a sequel to I: it examines the susceptibility given by the PF formula for the 2D OCP in a strip geometry for $\gamma = 2$. As announced in I, it is proved here that for both the transverse and parallel susceptibilities, the predictions of classical electrostatics and the results of statistical mechanics are rigorously identical in a shape-dependent thermodynamic limit. Furthermore, the dependence of the longitudinal susceptibility as a function of the distance between the pair of parallel lines defining the strip geometry is also given explicitly. Some algebraic details are given in the Appendix.

Section 7 deals with the case of the 2D OCP for $\gamma = 2$ and confined to the surface of a three-dimensional sphere. Using the SM formula, the susceptibility is given explicitly as a function of the number of particles. The saturation to the electrostatic value is reached with a first-order correction $O(N^{-1})$. The main result of this section is that for this unphysical but

boundary-free system, the SL sum rule is recovered in the thermodynamic limit.

2. DIELECTRIC CONSTANT AND SUSCEPTIBILITIES

In I we called the dielectric susceptibility tensor χ_Λ the tensor that relates the electric polarization density $\mathscr{P}$ of a Coulomb system in a domain Λ surrounded by vacuum to the applied field E_0. This tensor derives from the linear response theory of statistical mechanics, since the coupling of the system with the external field is $-P \cdot E_0$, where P is the instantaneous polarization. In phenomenological electrostatics[1,2] the dielectric susceptibility tensor χ_e is defined as the tensor that relates the electric polarization density $\mathscr{P}$ to the macroscopic or Maxwell field E acting in the system. While χ_Λ is shape-dependent, χ_e is shape-independent. For homogeneous systems the tensor χ_e reduces to a scalar quantity, whereas χ_Λ, althought generally diagonal, may be anisotropic.

In this section we recall the relations between the dielectric tensor ε, which relates the displacement field D to the field E and reduces to a scalar for isotropic systems, and the susceptibilities χ_e and χ_Λ of isotropic classical Coulomb systems for different shapes of interest, we discuss in some detail the Clausius–Mossotti relation,[3-5] and we give a heuristic argument concerning the fact that an OCP of appropriate shape satisfies the above relations in the plasma limit $\varepsilon = \infty$.

We consider, in two or three dimensions ($\nu = 2, 3$), a polarizable system of shape such that a uniform polarization produces a uniform depolarization field E_1; this is the case for elliptic ($\nu = 2$) and ellipsoidal ($\nu = 3$) domains, as proved in Refs. 6 and 7.

According to the above definitions and assumptions, we have the following equations:

$$\mathscr{P} = \chi_\Lambda E_0 \tag{2.1}$$

$$\mathscr{P} = \chi_e E \tag{2.2}$$

$$D = \varepsilon E \tag{2.3}$$

$$D = E + s_\nu \mathscr{P} \tag{2.4}$$

$$E = E_0 + E_1 \tag{2.5}$$

$$E_1 = -s_\nu T_\Lambda \mathscr{P} \tag{2.6}$$

where $s_\nu = 2^{\nu-1}\pi$ ($\nu = 2, 3$) and T_Λ is the depolarization tensor. With x a vector in $\mathbb{R}^\nu$, $|x|$ its norm, with the Coulomb potential $C_\nu(x) = -\ln|x|$,

and $|x|^{-1}$ respectively for $\nu = 2$ and 3, the components T_{Λ}^{ij} of this tensor are defined by (Ref. 7, p. 106)

$$T_{\Lambda}^{ij} = -(s_\nu)^{-1} \int_{\Lambda} d^\nu y \frac{\partial^2 C_\nu(y)}{\partial y_i \partial y_j} \tag{2.7}$$

or, for $x \subset \Lambda$, by

$$T_{\Lambda}^{ij}(x) = -(s_\nu)^{-1} \frac{\partial^2}{\partial x_i \partial x_j} \int_{\Lambda} d^\nu y \, C_\nu(x-y) \tag{2.8}$$

since the fundamental property of $T_{\Lambda}^{ij}(x)$ for elliptic or ellipsoidal domains is to be independent of x (Ref. 7, pp. 106–109). Analytic and numerical analysis of the components of T_{Λ}^{ij} for a general ellipsoid can be found in Refs. 8 and 9. In Section 5 the components T_{Λ}^{ij} for an ellipse are derived.

From Eqs. (2.2)–(2.4) we have the well-known relation

$$\varepsilon = \mathbb{1} + s_\nu \chi_e \tag{2.9}$$

where $\mathbb{1}$ is the unit tensor.

From Eqs. (2.2), (2.5), (2.6), and (2.1) we find the general and apparently new relation between χ_e and χ_Λ,

$$\chi_e = \chi_\Lambda (\mathbb{1} - s_\nu T_\Lambda \chi_\Lambda)^{-1} \tag{2.10}$$

We notice that for the strip ($\nu = 2$) or slab ($\nu = 3$) geometry χ_Λ possesses two types of components, $\chi_\perp$ and $\chi_{||}$, corresponding to E_0 perpendicular or parallel to the strip or slab and that in the latter case $\chi_{||} = \chi_e$, since $E = E_0$. From Eqs. (2.9) and (2.10) we find the relation between ε and χ_Λ,

$$\varepsilon = (\mathbb{1} - s_\nu T_\Lambda \chi_\Lambda)^{-1} [\mathbb{1} + s_\nu (\mathbb{1} - T_\Lambda) \chi_\Lambda] \tag{2.11}$$

At this point we wish to make a comment on the particular case where Λ is a ν-dimensional sphere (designated below by the symbol $\odot$). Here T_Λ is isotropic and we have $T_{\odot}^{ii} = \nu^{-1}$. For $\nu = 3$, Eq. (2.11) becomes

$$\varepsilon = (1 - 4\pi\chi_{\odot}/3)^{-1}(1 + 8\pi\chi_{\odot}/3) \tag{2.12}$$

This relation is manifestly the so-called Clausius–Mossotti relation between ε and the atomic polarizability α times the particle number density ρ.[1–5] This coincidence can be explained by the fact that for isotropic media and for a spherical geometry the external field E_0 equals the local field E_{loc} if the field produced by a mesoscopic, spherically symmetric

environment (the Lorentz cavity) of the atom singled out is zero or can be neglected. The general relations are indeed

$$\mathscr{P} = \alpha \rho E_{\text{loc}} \tag{2.13}$$

and, following the notation of Ref. 1, p. 455,

$$E_{\text{loc}} = E_0 + E_1 + E_2 + E_3 \tag{2.14}$$

where E_2 is the Lorentz (spherical) cavity field and E_3 the field of atoms inside the cavity. Since $E_2 = s_\nu T_\odot \mathscr{P}$,[3] we have, using Eq. (2.6) and with $E_3 = 0$,

$$E_{\text{loc}} = E_0 - s_\nu T_\Lambda \mathscr{P} + s_\nu T_\odot \mathscr{P} \tag{2.15}$$

and for a spherical Λ, $E_{\text{loc}} = E_0$, since $T_\Lambda = T_\odot$ is scale-invariant and $\chi_\odot = \alpha\rho$ according to Eq. (2.13).

A good candidate to test Mossotti's approximation ($E_3 = 0$) is Thomson's model of matter, which consists of a classical assembly of polarizable atoms where the electrons are point particles immersed in a neutralizing, homogeneous spherical ionic background. For a monoelectronic Thomson atom, the bounded electron is subject to an attractive potential $q^2 r^2 (2a^\nu)^{-1}$, where a is the radius of the ν-dimensional ionic sphere and the atomic polarizability is $\alpha = a^\nu$. It can be shown by symmetry arguments[1,3,10] that if the atoms are placed on a simple cubic lattice with overall spherical geometry, for example, and if the interactions between the Thomson atoms are approximated by their dipolar term, then $E_3 = 0$. Our conclusion is that Eq. (2.12) is much more general than the Clausius–Mossotti relation, since it is model-independent and free of any approximation.

The second comment to be made in this section concerns the plasma limit $\varepsilon \to \infty$ in Eq. (2.11). In this limit, the denominator of Eq. (2.11) vanishes and we find

$$\chi_\Lambda^P = (s_\nu T_\Lambda)^{-1} \tag{2.16}$$

In contrast, we recall the Stillinger–Lovett value $\chi_{\text{SL}}^P = (s_\nu)^{-1}$.

We wish now to present a heuristic argument for the fact that an OCP of appropriate shape has a susceptibility that satisfies Eq. (2.16) rather that the Stillinger–Lovett value.

The potential energy of an OCP consists of three parts: the particle–particle interaction V_{pp}, the particle–background interaction V_{pb}, and the self-energy of the background V_{bb}.

For V_{pb} we have by definition

$$V_{pb} = \sum_{n=1}^{N} (-)\, q^2 \rho_b \int_{\Lambda} d^\nu y\, C_\nu(x_n - y) \tag{2.17}$$

where ρ_b is the background density and N is the number of particles.

The point is that for elliptic or ellipsoidal domains, in using the identity

$$\begin{aligned}\int_{\Lambda} d^\nu y\, C_\nu(x-y) &= \int_{\Lambda} d^\nu y\, C_\nu(y) + \sum_{i=1}^{\nu} \int_0^{x_i} dx_i'' \int_0^{x_i''} dx_i' \frac{\partial^2}{\partial x_i'^2} \int_{\Lambda} d^\nu y\, C_\nu(x'-y) \\ &\quad + \sum_{1 \leqslant i < j \leqslant \nu} \int_0^{x_i} dx_i' \int_0^{x_j} dx_j' \frac{\partial^2}{\partial x_i' \partial x_j'} \int_{\Lambda} d^\nu y\, C_\nu(x'-y) \\ &= \int_{\Lambda} d^\nu y\, C_\nu(y) + \sum_{i=1}^{\nu} \int_0^{x_i} dx_i'' \int_0^{x_i''} dx_i' \left[-s_\nu T_{\Lambda}^{ii}(x')\right] \\ &\quad + \sum_{1 \leqslant i < j \leqslant \nu} \int_0^{x_i} dx_i' \int_0^{x_j} dx_j' \left[-s_\nu T_{\Lambda}^{ij}(x')\right]\end{aligned} \tag{2.18}$$

and in invoking the fundamental property [Eq. (2.8)] of the depolarization tensor, Eq. (2.17) becomes, as long as $x_n \subset \Lambda$, $\forall n$,

$$V_{pb} = -Nq^2\rho_b \int_{\Lambda} d^\nu y\, C_\nu(y) + \sum_{n=1}^{N} \sum_{i,j=1}^{\nu} \frac{1}{2} q^2 \rho_b s_\nu T_{\Lambda}^{ij} x_{n,i} x_{n,j} \tag{2.19}$$

The second term on the rhs of Eq. (2.19) is rewritten as follows:

$$\begin{aligned}&\sum_{n=1}^{N} \sum_{i,j=1}^{\nu} \frac{1}{2} q^2 \rho_b s_\nu T_{\Lambda}^{ij} x_{n,i} x_{n,j} \\ &\quad = \frac{1}{2N} \sum_{n,n'=1}^{N} \sum_{i,j=1}^{\nu} \frac{1}{2} q^2 \rho_b s_\nu T_{\Lambda}^{ij} (x_{n,i} x_{n,j} + x_{n',i} x_{n',j}) \\ &\quad = \frac{1}{2N} \sum_{n,n'=1}^{N} \sum_{i,j=1}^{\nu} \frac{1}{2} q^2 \rho_b s_\nu T_{\Lambda}^{ij} \\ &\qquad \times \left[(x_{n,i} - x_{n',i})(x_{n,j} - x_{n',j}) + x_{n,i} x_{n',j} + x_{n,j} x_{n',i}\right]\end{aligned} \tag{2.20}$$

It contains a translation-invariant part, which can be added to V_{pp}, and a non-translational-invariant part, which can be identified as a harmonic coupling of the center of mass $X = N^{-1} \sum_{n=1}^{N} x_n$ with the background. Introducing the plasma frequency $\omega_p = (s_\nu q^2 \rho_b / m)^{1/2}$, where m is the mass of the particles, this interaction becomes

$$V_{\mathrm{cm},b} = \sum_{i,j=1}^{\nu} \frac{N}{2} m \omega_p^2 T_{\Lambda}^{ij} X_i X_j \tag{2.21}$$

In terms of the center-of-mass coordinates, the components of the susceptibility tensor become, with $\rho = N/|\Lambda|$,

$$\chi_\Lambda^{ij} = \frac{\beta \langle P_i P_j \rangle}{|\Lambda|} = \frac{\beta q^2 N^2 \langle X_i X_j \rangle}{|\Lambda|}$$

$$= \beta q^2 \rho N \langle X_i X_j \rangle = \beta \frac{m\omega_p^2}{s_v} \frac{\rho}{\rho_b} N \langle X_i X_j \rangle \tag{2.22}$$

and since X decouples from the other degrees of freedom, the canonical average of Eq. (2.22) is asymptotically, with $\rho = \rho_b$ in the thermodynamic limit,

$$\chi_\Lambda^{ij} = s_v^{-1} (T_\Lambda^{-1})^{ij} \tag{2.23}$$

These are precisely the values required [Eq. (2.16)] by electrostatics. There is no shape for which the second-moment Stillinger–Lovett sum rule for plasmas is recovered. It is the purpose of Section 3 to explain this puzzling fact.

We end this section with a brief review of two equivalent expressions for the susceptibility: the polarization fluctuations (PF) and second moment (SM) formulas.

The PF formula derives from the linear response theory. Following the notations of I, we have the relations

$$\chi_{11,\Lambda} = \frac{\beta}{|\Lambda|} (\langle P_1^2 \rangle - \langle P_1 \rangle^2) \tag{2.24}$$

$$= \frac{\beta}{|\Lambda|} \int_\Lambda d^\nu x \int_\Lambda d^\nu y \, x_1 y_1 S_\Lambda(x, y) \tag{2.25}$$

$$= \frac{\beta}{|\Lambda|} \int_\Lambda d^\nu x \, d^\nu y \, x_1 y_1 \left[\sum_\alpha q_\alpha^2 \rho_{\alpha,\Lambda}(x) \, \delta(x-y) + \sum_{\alpha,\beta} q_\alpha q_\beta \rho_{\alpha\beta,\Lambda}^T(x, y) \right] \tag{2.26}$$

where P_1 is the x_1 component of the instantaneous polarization [I, Eq. (5)], $S_\Lambda(x, y)$ is the truncated charge–charge correlation function [I, Eq. (1)], $\rho_{\alpha,\Lambda}(x)$, $\rho_{\alpha\beta,\Lambda}(x, y)$, and $\rho_{\alpha\beta,\Lambda}^T(x, y)$ are the one-, two-, and truncated two-particle correlation functions, and α and β label the species of the system considered.

The SM formula is obtained from Eq. (2.25) by writing

$$x_1 y_1 = -\frac{1}{2}(y_1 - x_1)^2 + \frac{1}{2}(y_1^2 + x_1^2)$$

Noticing that the contributions of the last two terms cancel since

$$\int_{\Lambda} dx\, S_{\Lambda}(x, y) = \int_{\Lambda} dy\, S_{\Lambda}(x, y) = 0$$

for both neutral and charged systems, we have

$$\chi_{11,\Lambda} = -\frac{1}{2}\frac{\beta}{|\Lambda|}\sum_{\alpha,\beta} q_\alpha q_\beta \int_{\Lambda} d^\nu x\, d^\nu y\, (y_1 - x_1)^2\, \rho^T_{\alpha\beta,\Lambda}(x, y) \tag{2.27}$$

The SM formula is an example of the expectation value of an observable which is (i) translationally invariant and (ii) unbounded.

The first property suggests introducing the relative coordinates $r = y - x$ and defining the pair correlation function

$$\bar{\rho}_{\alpha\beta,\Lambda}(r) = \frac{1}{|\Lambda|}\int_{D_\Lambda(r)} d^\nu x\, \rho^T_{\alpha\beta,\Lambda}(x, x + r) \tag{2.28}$$

where the domain of integration $D_\Lambda(r)$ is such that $x \subset \Lambda$ and $x + r \subset \Lambda$. If Λ_r designates the domain Λ shifted by the vector r, then $D_\Lambda(r) = \Lambda \cap \Lambda_r$. For example, if Λ is a disk of radius R, then $D_\Lambda(r)$ is the lunular region defined by the intersection of two disks having their center separated by a distance $|r|$. With Eq. (2.28) we can write Eq. (2.27) in the form

$$\chi_{11,\Lambda} = -\frac{\beta}{2}\sum_{\alpha,\beta} q_\alpha q_\beta \int_{\Omega_\Lambda} d^\nu r\, r_1^2 \bar{\rho}_{\alpha\beta,\Lambda}(r) \tag{2.29}$$

where the domain of integration Ω_Λ is obtained as follows: let O, chosen as the origin, be any point of Λ, let P be any point on the boundary $\partial\Lambda$ of Λ, and let Λ_P be the domain Λ shifted by the vector PO (to the origin); then Ω_Λ is generated by $\bigcup \Lambda_P$, $\forall P \subset \partial\Lambda$. Some examples are: if Λ is a square of side length L, then Ω_Λ is a square of side length $2L$; if Λ is an equilateral triangle of side length L, then Ω_Λ is a hexagon of side length L; if $\Lambda = S(R)$ is a disk of radius R, then $\Omega_\Lambda = S(2R)$ is a disk of radius $2R$.

The second property of the observable r^2, namely the fact that it is unbounded, suggests introducing the concept of partial second moment, an object that should permit us to examine the contributions to the total susceptibility of pairs of particles of increasing separation. This partial second moment is defined as follows: let $\lambda \in]0; 1]$ be a scaling parameter and $\lambda\Omega_\Lambda$ be a shape similar subdomain of Ω_Λ; then

$$\chi_{11,\Lambda}(\lambda) = -\frac{\beta}{2}\sum_{\alpha,\beta} q_\alpha q_\beta \int_{\lambda\Omega_\Lambda} d^\nu r\, r_1^2 \bar{\rho}_{\alpha\beta,\Lambda}(r) \tag{2.30}$$

For example, if Λ is a disk or sphere of radius R, then $\lambda = |r|/2R$. The central question to which this paper is addressed can now be taken up.

3. THE OCP ON A DISK FOR $\gamma = 2$

For the OCP on a disk of radius R_b the one- and two-particle correlation functions will be relabeled $\rho_{1,\odot}(x)$ and $\rho_{2,\odot}(x, y)$. For this isotropic model, Eqs. (2.28)–(2.30) become, respectively,

$$\bar{\rho}_{2,\odot}(r) = (\pi R_b^2)^{-1} \int_{D_\odot(|r|)} d^2x\, \rho^T_{2,\odot}(x, x+r) \tag{3.1}$$

$$\chi_{11,\odot} = -\frac{1}{4}\gamma \int_{S(2R_b)} d^2r\, r^2 \bar{\rho}_{2,\odot}(r) \tag{3.2}$$

$$\chi_{11,\odot}(r) = -\frac{1}{4}\gamma \int_{S(|r|)} d^2r'\, r'^2 \bar{\rho}_{2,\odot}(r') \tag{3.3}$$

In this geometry $\rho_{2,\odot}(x, y)$ is invariant upon reflection and rotation. This means that $\rho_{2,\odot}(x, y)$ is a function of $|x|$, $|y|$, and $|\theta|$, where θ is the angle between y and x, or is a function of $|x|$, $|y|$, and $|r|$, where

$$|r|^2 = |x|^2 + |y|^2 - 2\,|x|\,|y| \cos|\theta|$$

This property suggests determining $\bar{\rho}_{2,\odot}(r)$, which will be a function of $|r|$, from an integral representation using $|x|$, $|y|$, and $|r|$ as independent variables. Let $s = |r|$ and α, $u = |x|$ and φ, and $v = |y|$ and ψ be the polar coordinates of r, x, and y. We change the system of coordinates (φ, ψ, u, v) into (α, s, u, v) via the system (α, θ, u, v). Noticing that the Jacobian $\partial(\varphi, \psi)/\partial(\alpha, \theta) = 1$, we have

$$\begin{aligned} d^2x\, d^2y &= d\varphi\, d\psi\, u\, du\, v\, dv \\ &= d\alpha\, d\theta\, u\, du\, v\, dv \\ &= 2\, d\alpha\, d|\theta|\, u\, du\, v\, dv \\ &= 2\, d\alpha\, s\, ds \frac{d|\theta|}{s\, ds} u\, du\, v\, dv \\ &= d^2r \frac{2\, du\, dv}{\sin|\theta|}; \qquad \theta \in [0; \pi] \\ &= d^2r \frac{2u\, du\, v\, dv}{[u^2v^2 - \frac{1}{4}(u^2 + v^2 - s^2)^2]^{1/2}} \end{aligned} \tag{3.4}$$

The domain of integration in the (u, v) plane, called $D'_\odot(s)$, is given by the intersection of the square $v = 0$, $u = R_b$, $v = R_b$, $u = 0$ with the semiinfinite

strip $v+u=s$, $v=u+s$, and $v=u-s$. The last three equations are solutions of $\sin|\theta|=0$, i.e.,

$$\begin{aligned}4u^2v^2-(u^2+v^2-s^2)=0&=[2uv-(u^2+v^2-s^2)][2uv+(u^2+v^2-s^2)]\\&=[s^2-(v-u)^2][(u+v)^2-s^2]\\&=(s+v-u)(s-v+u)(u+v-s)(u+v+s)\end{aligned}\tag{3.5}$$

The domain $D'_{\odot}(s)$ is the image of that half of $D_{\odot}(s)$, the lunular domain cut into two halves by the line joining the centers of the two circles $S(R)$ and $S_r(R)$, for which $\theta\in[0;\pi]$. We have the relations

$$\begin{aligned}|D_{\odot}(s)|=\int_{D_{\odot}(s)}d^2x&=2\int_{D'_{\odot}(s)}\frac{du\,dv}{\sin|\theta|}=2\,|D'_{\odot}(s)|\\&=2R_b^2\left\{\arccos\left(\frac{s}{2R_b}\right)-\left(\frac{s}{2R_b}\right)\left[1-\left(\frac{s}{2R_b}\right)^2\right]^{1/2}\right\}\end{aligned}\tag{3.6}$$

and we define the ratio

$$\Delta\left(\frac{s}{2R_b}\right)=|D_{\odot}(s)|\,(\pi R_b^2)^{-1}\tag{3.7}$$

In this new integral representation Eqs. (3.1) and (3.3) become, respectively,

$$\bar{\rho}_{2,\odot}(s)=(\pi R_b^2)^{-1}\int_{D'_{\odot}(s)}\frac{2\,du\,dv}{\sin|\theta(u,v,s)|}\,\rho^T_{2,\odot}(u,v,s)\tag{3.8}$$

and for $s\in\,]0;2R_b]$

$$\chi_{11,\odot}(s)=-\frac{\gamma}{4}\frac{2\pi}{\pi R_b^2}\int_0^s ds'\,s'^3\int_{D'_{\odot}(s')}\frac{2\,du\,dv}{\sin|\theta|}\,\rho^T_{2,\odot}(u,v,s')\tag{3.9}$$

Our next purpose is to establish approximations of $\rho^T_{2,\odot}(u,v,s)$ suited to analyze the behavior of the partial second moment. Particular attention will be paid to the s dependence of this correlation function when both u and v are close to $R=(N/\pi\rho_b)^{1/2}$, where N is the number of particles. This purpose has been achieved for $\gamma=2$ in the case where the incomplete gamma functions $\gamma(l+1,M)$ that enter in the definition of $\rho^T_{2,\odot}$ [I, Eq. (12)] are approximated by their upper bound $\gamma(l+1,\infty)=l!$. This is a very good approximation for the important values of l, which are close to N if there is a positive excess background charge $S(N)$ such that $S(N)/N^{1/2}\to\infty$ as $N\to\infty$, while $S(N)/N\to 0$ as $N\to\infty$ in order to give a mean-

ing to the thermodynamic limit of the susceptibility $\chi(N, M)$ given by I, Eq. (12). For example, an excess charge $S(N) = N^{3/4}$ will satisfy both conditions and the radius of the background will be given by $\pi\rho_b R_b^2 = N + S(N)$, i.e., $R_b \approx (\pi\rho_b)^{-1/2}(N^{1/2} + \frac{1}{2}N^{1/4})$.

Following the notations of I, we set $u = (\pi\rho_b)^{-1/2}|z|$, $v = (\pi\rho_b)^{-1/2}|z'|$, $s = (\pi\rho_b)^{-1/2}|z - z'|$, and

$$\rho^T_{2,\odot}(u, v, s) = \rho_b^2 h_N(z, z') \tag{3.10}$$

With our assumptions and if we set $N - 1 = n$ we have

$$-h_N(z, z') = \exp(-|z|^2 - |z'|^2)\, K_n(zz'^*)\, K_n(z^* z') \tag{3.11}$$

where, setting $w = zz'^*$,

$$K_n(w) = \sum_{l=0}^{n} \frac{w^l}{l!} \tag{3.12}$$

We write Eq. (3.12) in the following integral representations:

$$\begin{aligned} K_n(w) &= K_\infty(w) - \sum_{l=n+1}^{\infty} \frac{w^l}{l!} \\ &= e^w - \frac{1}{n!} e^w \int_0^w dt\, t^n e^{-t} \\ &\equiv e^w - L_n(0, w) \end{aligned} \tag{3.12a}$$

and

$$K_n(w) = \frac{1}{n!} e^w \int_w^\infty dt\, t^n e^{-t} \equiv L_n(w, \infty) \tag{3.12b}$$

respectively useful for $|w| < n$ and $|w| > n$. We proceed with partial integrations of Eqs. (3.12a) and (3.12b), namely

$$\begin{aligned} L_n(0, w) &= \frac{1}{n!} \frac{w^{n+1}}{n - w} - \frac{e^w}{n!} \int_0^w dt \frac{n}{(n-t)^2} t^n e^{-t} \\ &\equiv \frac{1}{n!} \frac{w^{n+1}}{n - w} - R_n(0, w) \end{aligned} \tag{3.13a}$$

and

$$\begin{aligned} L_n(w, \infty) &= \frac{1}{n!} \frac{w^{n+1}}{w - n} - \frac{e^w}{n!} \int_w^\infty dt \frac{n}{(n-t)^2} t^n e^{-t} \\ &\equiv \frac{1}{n!} \frac{w^{n+1}}{w - n} - R_n(w, \infty) \end{aligned} \tag{3.13b}$$

With the help of the above representations and asymptotic expansions, the function $h_N(z, z')$ will be described in the following situations: (a) both z and z' are in the interior of the circle of radius $\sqrt{N}$; (b) one is in the interior and the other in the exterior; (c) both are in the exterior.

If, for reasons to become clear later, we neglect the remainders $R_n(0, w)$ and $R_n(w, \infty)$, we obtain for the three situations considered above

$$-h_N^{(a)}(z, z') \approx \exp(-|z|^2 - |z'|^2)\left(\exp(w) - \frac{1}{n!}\frac{w^{n+1}}{n-w}\right) \times \left(\exp(w^*) - \frac{1}{n!}\frac{(w^*)^{n+1}}{n-w^*}\right) \tag{3.14a}$$

$$-h_N^{(b)}(z, z') \approx \exp(-|z|^2 - |z'|^2)\left(\exp(w) - \frac{1}{n!}\frac{w^{n+1}}{n-w}\right)\frac{1}{n!}\frac{(w^*)^{n+1}}{w^*-n} + \text{c.c} \tag{3.14b}$$

$$-h_N^{(c)} \approx \exp(-|z|^2 - |z'|^2)\left(\frac{1}{(n!)^2}\frac{ww^*(ww^*)^n}{(w-n)(w^*-n)}\right) \tag{3.14c}$$

where c.c. means complex conjugate.

Inspection of these equations reveals the existence of two distinct behaviors of $h_N(z, z')$ corresponding, respectively, to a bulk behavior and a surface behavior. The first is given by the product of the first two terms of Eq. (3.14a). We find the well-known formula for the infinite OCP at $\gamma = 2$, namely,

$$-h_N^{\text{bulk}}(z, z') = \exp(-|z - z'|^2) \tag{3.15}$$

Following Eq. (3.10), we have

$$\rho_{2,\odot}^{T,\text{bulk}}(s) = -\rho_b^2 \exp(-\pi\rho_b s^2) \tag{3.16}$$

and according to Eqs. (3.6)–(3.8)

$$\bar{\rho}_{2,\odot}^{\text{bulk}}(s) = -\Delta(s/2R_b)\,\rho_b^2 \exp(-\pi\rho_b s^2) \tag{3.17}$$

Following Eq. (3.3), we can calculate the bulk contribution to the partial second moment, namely

$$\chi_{11,\odot}^{\text{bulk}}(s) = \frac{1}{2}\cdot 2\pi\rho_b^2 \int_0^s ds'\, s'^3 \Delta\left(\frac{s'}{2R_b}\right)\exp(-\pi\rho_b s'^2)$$
$$= \frac{1}{2\pi} - \frac{1}{2\pi}(1 + \pi\rho_b s^2)\exp(-\pi\rho_b s^2)\left[1 - O\left(\frac{s}{R_b}\right)\right] \tag{3.18}$$

We observe that, for $\pi\rho_b s^2 < 1$, $\chi^{\text{bulk}}_{11,\odot}(s) \approx (1/2\pi)\cdot\frac{1}{2}(\pi\rho_b s^2)^2$, whereas for $\pi\rho_b s^2 > 1$, $\chi^{\text{bulk}}_{11,\odot}(s)$ saturates rapidly to $1/2\pi$. As expected, the bulk part of the second moment yields the Stillinger–Lovett value.

The surface part of $h_N(z, z')$ is composed either of Eq. (3.14c) or of the second term of Eq. (3.14b) or its complex conjugate or of the fourth term of Eq. (3.14a), depending on the location of $|z|$ and $|z'|$ with respect to the circle of radius $\sqrt{N}$. Since these four parts are algebraically identical, they can be lumped together by analytic continuation, except at $w = n$, and we obtain

$$-h_N^{\text{surface}}(z, z') = \exp(-|z|^2 - |z'|^2)\frac{ww^*(ww^*)^n}{|w-n|^2(n!)^2} \tag{3.19}$$

Equation (3.19) is valid for $|z|$ and $|z'|$ in the neighborhood of the circle of radius $\sqrt{N}$. Let us proceed with an analysis of Eq. (3.19). Its denominator can be written as follows:

$$\begin{aligned} |n-w|^2 &= n^2 - nzz'^* - nz^*z' + zz^*z'z'^* \\ &= (n-|z|^2)(n-|z'|^2) + n\,|z-z'|^2 \\ &= (n-\pi\rho_b u^2)(n-\pi\rho_b v^2) + n\pi\rho_b s^2 \end{aligned} \tag{3.20}$$

Thus, following Eq. (3.10),

$$\begin{aligned} -\rho^{T,\text{surface}}_{2,\odot}(u, v, s) = \rho_b^2 \exp[-\pi\rho_b(u^2+v^2)]\frac{(\pi\rho_b u^2)^n}{n!}\frac{(\pi\rho_b v^2)^n}{n!} \\ \times\frac{(\pi\rho_b)^4 u^2 v^2}{(n-\pi\rho_b u^2)(n-\pi\rho_b v^2) + n\pi\rho_b s^2} \end{aligned} \tag{3.21}$$

Using the Stirling formula $n! \approx (2\pi n)^{1/2}\exp(n\ln n - n)$, we observe that the first three terms of Eq. (3.21) take the form

$$F_n(u, v) = \frac{1}{2\pi n}\exp(n-\pi\rho_b u^2)\left(\frac{\pi\rho_b u^2}{n}\right)^n \exp(n-\pi\rho_b v^2)\left(\frac{\pi\rho_b v^2}{n}\right)^n \tag{3.22}$$

It is apparent that the above function is sharply peaked around $\pi\rho_b u^2 = \pi\rho_b v^2 = n$. For these particular values, we find

$$\begin{aligned} -\rho^{T,\text{surface}}_{2,\odot}\left(\left(\frac{n}{\pi\rho_b}\right)^{1/2}, \left(\frac{n}{\pi\rho_b}\right)^{1/2}, s\right) &= \rho_b^2\frac{n^2}{n\pi\rho_b s^2}\frac{1}{2\pi n} \\ &= \frac{1}{2\pi^2}\frac{\rho_b}{s^2} = \frac{1}{2\pi^2}\frac{\rho_b}{|r|^2} \end{aligned} \tag{3.23}$$

Equation (3.23) displays a fundamental property of $\rho_{2,\odot}^{T,\text{surface}}(|r|)$, that it decays as $|r|^{-2}$ for large $|r|$. The qualitative expectation that near the surface of the OCP perfect screening breaks down and that dipolar interaction dominates is thus demonstrated. At this point the fact that the remainders $R_n(0, w)$ and $R_n(w, \infty)$ have been neglected can be justified: the next integration by parts produces the term

$$R_n = -\frac{w^n}{n!}\left[\frac{nw}{(n-w)^3} + O\left(\frac{n^3}{(n-w)^s}\right)\right] \tag{3.24}$$

For $w = ne^{-i\theta}$ the correction to Eq. (3.23) becomes

$$(\rho_b/2\pi^2 s^2)(4/n)(1 - 2/\pi\rho_b s^2)$$

which is indeed negligible for large n and for $s > 0$.

We are ready to calculate the surface contribution to the partial second moment given by Eq. (3.9). Introducing the new variables ξ, η, and ρ through $u = (n/\pi\rho_b)^{1/2}(1+\xi)$, $v = (n/\pi\rho_b)^{1/2}(1+\eta)$, and $|r| = s = (n/\pi\rho_b)^{1/2}\rho = R\rho$ with $\pi\rho_b R^2 = n$, expanding $\ln(1+\xi) = \xi - \frac{1}{2}\xi^2 + O(\xi^3)$ and similarly for $\ln(1+\eta)$, we find

$$-\rho_{2,\odot}^{T,\text{surface}}(\xi, \eta, \rho) = \rho_b^2 \exp\{-2n[\xi^2 + \eta^2 + O(\xi^3) + O(\eta^3)]\} \cdot (2\pi n)^{-1} \times \frac{(1+\xi)^2(1+\eta)^2}{[1-(1+\xi)^2][1-(1+\eta)^2] + \rho^2} \tag{3.25}$$

For the volume element we find next

$$2\pi s\, ds \frac{2\, du\, dv}{\sin|\theta|} = \frac{8\pi n^2}{(\pi\rho_b)^2} \frac{\rho(1+\xi)(1+\eta)\, d\rho\, d\xi\, d\eta}{\{[\rho^2 - (\eta-\xi)^2][(2+\xi+\eta)^2 - \rho^2]\}^{1/2}} \tag{3.26}$$

For the partial second moment we find lastly, recalling that $\pi\rho_b R_b^2 = M = N + S(N)$, that $n = N - 1$ and $\gamma = 2$,

$$\chi_{11,\odot}^{\text{surface}}(\rho) = \frac{N-1}{\pi^2 M}\int_0^\rho d\rho'\, \rho' \int_{D'_\odot(\rho')} d\xi\, d\eta \times \frac{(1+\xi)^3(1+\eta)^3}{[\rho'^2 - (\eta-\xi)^2]^{1/2}[(2+\xi+\eta)^2 - \rho'^2]^{1/2}} \times \frac{\rho'^2}{[1-(1+\xi)^2][1-(1+\eta)^2] + \rho'^2} \times \frac{2(N-1)}{\pi} \exp\{-2(N-1)[\xi^2 + \eta^2 + O(\xi^3) + O(\eta^3)]\} \tag{3.27}$$

At this point we note that thanks to the term ρ'^2 in the numerator of the integrand, we can take the limit $N \to \infty$ under the integrals. This limit produces the product of Dirac distributions $\delta(\xi)\,\delta(\eta)$. Thus, with $\rho = s/R$ varying from 0 to 2, we have, since $N/M \to 1$,

$$\chi_{11,\odot}^{\text{surface}}(\rho) = \frac{1}{\pi^2}\int_0^{\rho} d\rho' \frac{1}{(4-\rho'^2)^{1/2}} = \frac{1}{\pi^2}\arcsin\left(\frac{\rho}{2}\right) \tag{3.28}$$

This is a new and exact result, which tells us how the surface contribution to the total susceptibility reaches the value $1/2\pi$, which together with the bulk contribution of $1/2\pi$ yields the result of $1/\pi$ obtained in I, Eq. (16). Equation (3.28) will be designated as the "arc sine" law.

It remains to show that the interference terms not considered so far have no effect for large systems. They are the cross-terms of Eqs. (3.14a) and (3.14b), namely

$$-h_N^{\text{interf}}(z, z') \approx \exp(-|z|^2 - |z'|^2 + w)\frac{1}{n!}\frac{(w^*)^{n+1}}{w^* - n} + \text{c.c} \tag{3.29}$$

$$= \exp(-|z|^2 - |z'|^2 + |z|\,|z'|\cos\theta)\frac{(|z|\,|z'|^n}{n!}\frac{|z|\,|z'|}{|zz'^* - n|}\,2\cos\phi \tag{3.30}$$

where

$$\phi(|z|, |z'|, \theta, n) = -|z|\,|z'|\sin\theta + (n+1)\,\theta + \operatorname{arctg}\frac{|z|\,|z'|\sin\theta}{|z|\,|z'|\cos\theta - n} \tag{3.31}$$

We observe that the amplitude of Eq. (3.30) is twice the square root of $h_N^{\text{bulk}}(z, z')$ times $h_N^{\text{surface}}(z, z')$ of Eqs. (3.15) and (3.19). Ignoring the rapidly oscillating phase factor in Eq. (3.30), we can give an upper bound estimate to the partial SM of the interference terms. Using the Stirling formula, we have, with Eq. (3.22),

$$\chi_{11,\odot}^{\text{interf}}(s) \leqslant 2\frac{2\pi}{\pi R_b^2}\rho_b^2\int_0^s ds' \times s'^3 \int_{D'_{\odot}(s')} \frac{2\,du\,dv}{\sin|\theta|}\frac{(\pi\rho_b)^2\,uv}{[(n-\pi\rho_b u^2)(n-\pi\rho_b v^2) + n\pi\rho_b s^2]^{1/2}} \times \exp\left(-\frac{1}{2}\pi\rho_b s^2\right)\cdot F_n^{1/2}(u, v) \tag{3.32}$$

Introducing again the variables ρ, ξ, and η and symmetrizing the integration over ρ', we have that Eq. (3.32) becomes

$$\chi_{11,\odot}^{\text{interf}} \leqslant \frac{1}{\pi}\frac{n}{M}\int_{-\rho}^{\rho} d\rho' \, |\rho'|^3 \times \int_{D'_{\odot}(|\rho'|)} d\xi \, d\eta \, \frac{(1+\xi)^2(1+\eta)^2}{[\rho'^2-(\eta-\xi)^2]^{1/2}[(2+\xi+\eta)^2-\rho'^2]^{1/2}} \times \frac{1}{\{[1-(1+\xi)^2][1-(1+\eta)^2]+\rho'^2\}} \times \frac{n^2}{\pi(2\pi n)^{1/2}} \exp\left(-\frac{1}{2}n\rho'^2 - n\xi^2 - n\eta^2\right) \tag{3.33}$$

It is apparent that the limit $n \to \infty$ produces the product of three Dirac distributions $\delta(\rho)\,\delta(\xi)\,\delta(\eta)$; thus,

$$\chi_{11,\odot}^{\text{interf}}|_{n\to\infty} \leqslant \frac{1}{\pi}\int_{-\rho}^{\rho} d\rho' \frac{|\rho'|}{4-\rho'^2}\,\delta(\rho') = 0 \tag{3.34}$$

For n large but finite it is easy to show from Eq. (3.33) that $\chi_{11,\odot}^{\text{interf}}(\rho) \leqslant O(n^{-1/2})$. We are now confident that the partial second moment is additively made up of a bulk and a surface contribution and thus that the final result of this section reads, with $\rho_b = \rho$ the particle density and $R_b = R$ for macroscopic systems

$$\chi_{11,\odot}(|r|) = \frac{1}{2\pi} - \frac{1}{2\pi}(1+\pi\rho\,|r|^2)\exp(-\pi\rho\,|r|^2) + \frac{1}{\pi^2}\arcsin\left(\frac{|r|}{2R}\right) \tag{3.35}$$

4. NUMERICAL RESULTS AND MONTE CARLO SIMULATIONS

This section presents exact numerical results for the OCP on a disk for $\gamma = 2$ and some results obtained by Monte Carlo (MC) simulations for an OCP and a TCP for $\gamma = 2$ and at other temperatures.

Figure 1 shows the $1/r^2(|z|, |z'|, \theta)$ dependence of the exact two-particle correlation function $h(z, z')$ defined by I, Eq. (12) divided by ρ_b^2 for two different distances from the edge. The absolute values of z and z' are kept fixed and the angle θ is varied from 0 to π. Since the figure represents $-|z-z'|^2\,h(z, z')$, the plots are expected to be flat for large separations, as indicated by the analytical approximation [Eq. (3.23)]. Indeed, the function is completely flat even for short separations. This behavior remains qualitatively the same when both $|z|$ and $|z'|$ are at larger distances

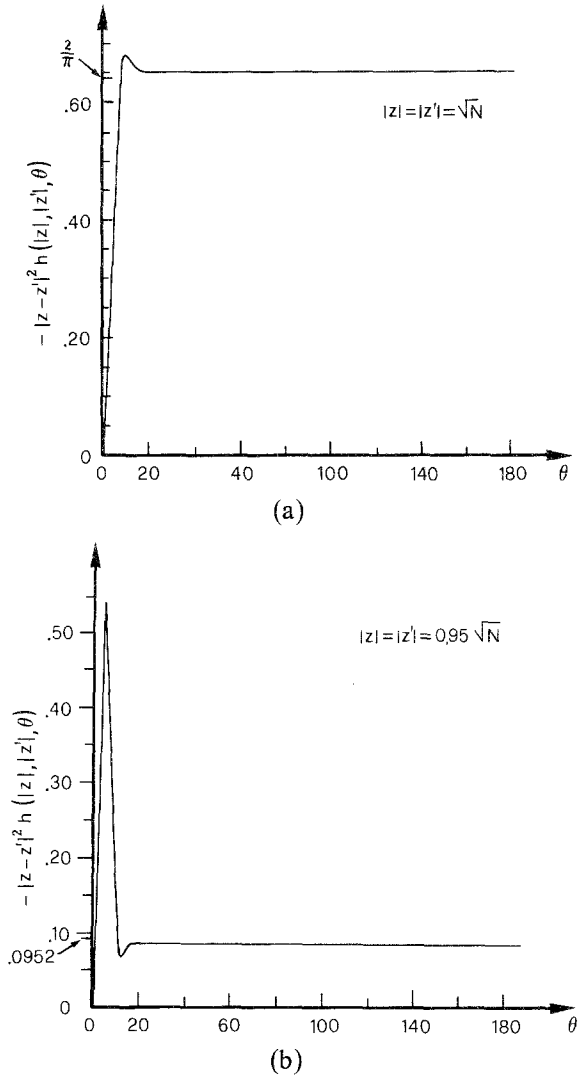

Fig. 1. (a) The $1/|r|^2$ decay of the correlation function on the edge, $|z| = |z'| = \sqrt{N}$. The function $h(|z|, |z'|, \theta)$ is multiplied by the square of the distance $|z - z'|^2$. The amplitude of the correlation function (on the edge) is in good agreement with the asymptotic value of $2/\pi$ given in Ref. 13 (Eq. 2.21). (b) The same plot as (a), except that $|z| = |z'| = 0.95\sqrt{N}$. The asymptotic value is given by $(2/\pi)\exp(-2 \cdot 0.95) = 0.0952$.

from the edge, but the amplitude is now much smaller. Even for small N, the amplitude of the function is very close to $2/\pi$, the value of the infinite-system solution, which can be inferred from the result established by Jancovici for the truncated pair correlation function of an OCP near a wall [Ref. 13, Eq. (2.21)] and which differs from Eq. (3.23) by a factor of 4. The difference between the two systems is that in I, Eq. (12) and in the simulations, we have strict neutrality and a strong influence of the edge, whereas in Eq. (3.11), which leads to Eq. (3.23) in the limit of an infinite system, the background has a positive excess charge and the particles can move beyond the radius $(N/\pi\rho_b)^{1/2}$. The difference in the normalization of the respective truncated correlation functions accounts exactly for this factor 4.

In Eq. (2.28) we have defined a pair correlation function depending on the relative position vector r. Since this function is not naturally obtained in a computer simulation, we have used the radial pair correlation, which is the pair correlation function integrated over the angle, i.e.,

$$\hat{\rho}_{2,\odot}(|r|) = \int_0^{2\pi} d\theta\, |r|\, \bar{\rho}_{2,\odot}(|r|, \theta) \tag{4.1}$$

For a spherical geometry, this operation amounts to multiplying Eq. (2.28) by $2\pi\,|r|$.

Figure 2 shows this radial pair correlation function obtained from the exact two-point correlation function [I, Eq. (12)] with 44 particles. The

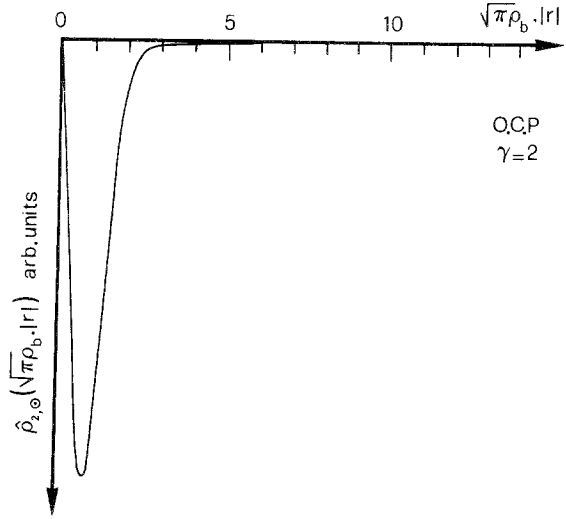

Fig. 2. Radial pair correlation function for $\gamma = 2$ and $N = 44$ obtained from the exact truncated two-body-correlation function of the model.

function starts at 0 and not at -1, as one would expect for the pair correlation function, because of the integration over the angle. Even at large distances, the function stays slightly negative because of the strong negative correlation near the surface.

For temperatures other than $\gamma = 2$, we used MC simulations to determine the truncated correlation functions. One of the reasons we finally chose MC simulations rather than molecular dynamics was the following, very annoying behavior of the OCP. The degree of freedom of the center of mass (which is also the electric moment) is coupled to the other degrees only via collisions of the particles with the wall. We have observed that the motion of the center of mass did not thermalize fast enough at low temperature, and therefore the time averages were not representative. How did we compute the radial pair correlation function $\hat{\rho}_{2,\odot}(|r|)$? This function is defined by

$$\hat{\rho}_{2,\odot}(|r|) = \int |r|\, d\theta \frac{1}{\pi R_b^2} \int_{D_\odot(|r|)} d^2x\, \rho_{2,\odot}(x, x+r) - \int |r|\, d\theta \frac{1}{\pi R_b^2} \int_{D_\odot(|r|)} d^2x\, \rho_{1,\odot}(x)\, \rho_{1,\odot}(x+r) \tag{4.2}$$

We have to compute in a first step the usual pair correlation function and then subtract the product of the densities. Since the truncated pair correlation function is the difference of two large functions, we need very high precision and therefore extremly good statistics in order to obtain a function with an error smaller than the function itself. This goal can of course not be achieved with reasonable computer time, but we have used a method that at least suppresses all systematic errors. When we calculate the convolution of the one-particle densities, we do not use in the integral a systematic sampling of the space, but we make a statistical approach. The idea basically consists in generating totally uncorrelated configurations with the same average density as the real system. The convolution of the densities is computed in exactly the same way as the real pair correlation function. This ensures that the result converges to the exact one for a long enough run. Still, we had to sample runs of almost one million moves per particle for 44 particles to obtain reasonably accurate results.

Figure 3 represents $\hat{\rho}_{2,\odot}(|r|/R_b)$ of a system of 44 particles for $\gamma = 1.5$ and Fig. 4 represents the partial second moment for a system of 44 particles for $\gamma = 2$. The smooth line is the exact solution, the noisy one is the result of the MC simulations. We encountered more and more difficulties when we increased the number of particles, especially at low temperature. For 100 or more particles, the partial second moment had the correct behavior for short distances. At large separations, the noise level was so great that

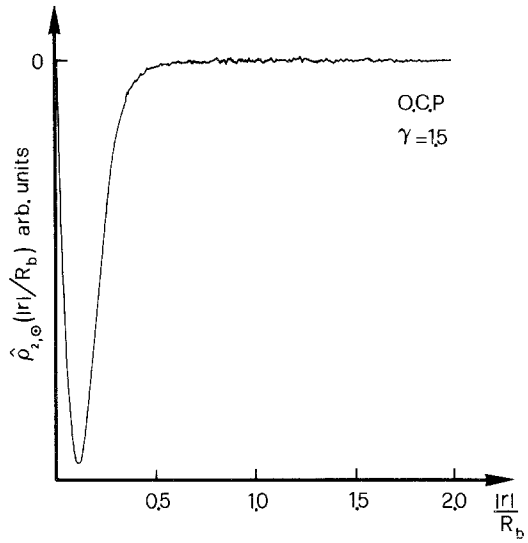

Fig. 3. Radial pair correlation function for $\gamma = 1.5$ and for $N = 44$ obtained by MC simulation.

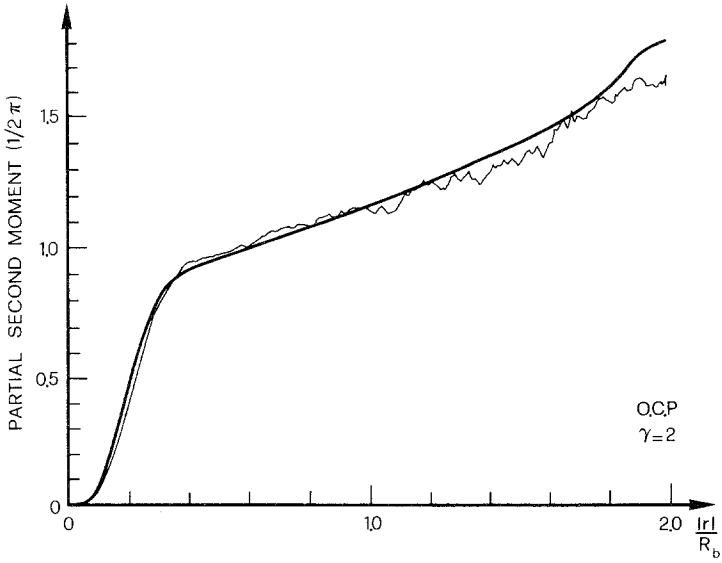

Fig. 4. Partial second moment obtained from the exact pair correlation function (smooth curve) and from MC simulation (noisy curve).

the partial second moment reached a completely wrong value at $2R$. However, since the MC and analytical results agree for $\gamma = 2$ and for a small number of particles, we can assume that the MC results are also reliable at other temperatures and for other systems, provided that the statistics are good enough.

Figure 5 represents the partial second moment of a subdomain of a system with 100 particles. It is obtained from the exact solution for $\gamma = 2$, where one includes in the integral only particles inside a disk of radius αR $(0 < \alpha \leqslant 1)$ and where the normalization is also the area of the subdomain. The radii are respectively $1.0R$, $0.97R$, $0.95R$, and $0.9R$. We notice that the surface contribution is restricted to a very thin layer.

Figure 6 shows the radial pair correlation function for 44 particles for $\gamma = 4$, and Fig. 7 the partial second moment for $\gamma = 4$. The curve confirms the "arc sine" behavior of the surface part. Note the hump in the radial correlation function and in the partial second moment. This hump is due to the presence of short-range order, which is known to set in at $\gamma = 2$ and is amplified by the partial second moment.

Since the OCP is in a certain sense a rather pathological system, we wanted to check if a more realistic Coulomb system with only pair interac-

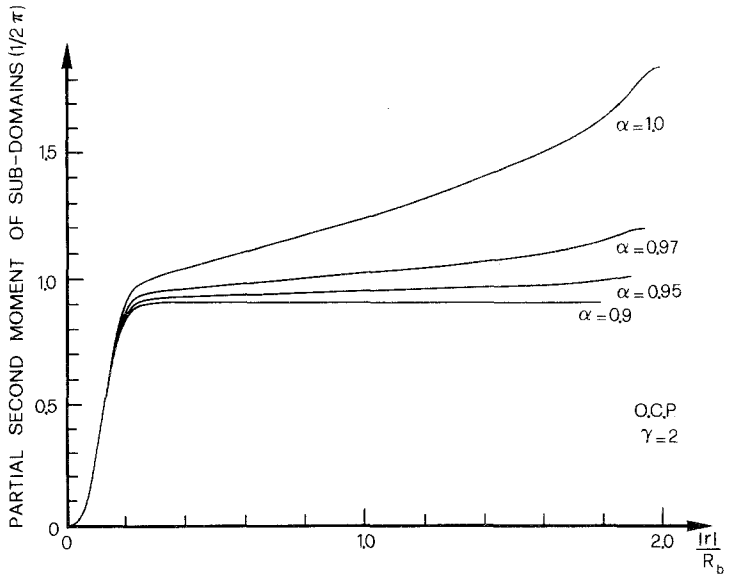

Fig. 5. Partial second moment of circular subdomains with radii αR for $\alpha = 1.0$, 0.97, 0.95, 0.9.

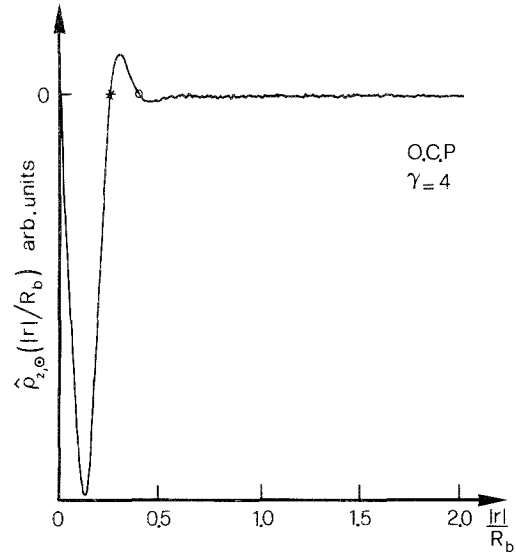

Fig. 6. Radial pair correlation function for $\gamma = 4$ and $N = 44$ obtained by MC simulation.

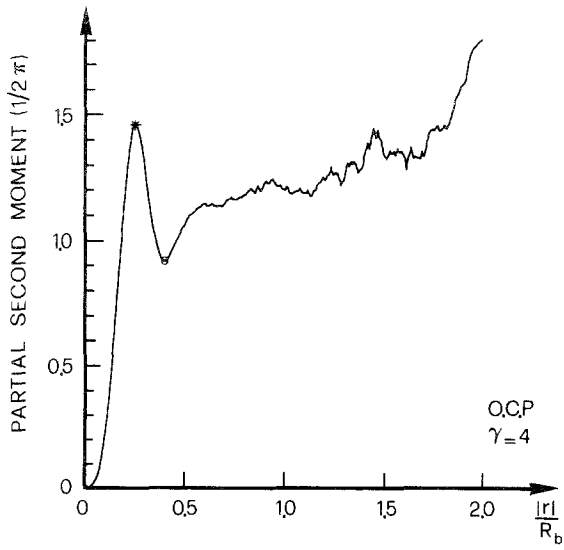

Fig. 7. Partial second moment for $\gamma = 4$ and for $N = 44$ obtained by MC simulation. Note the local extrema indicated by (*, ○) and the corresponding points on Fig. 6.

tions exhibits the same behavior as the OCP. Of particular interest is the question of whether the partial SM in a general Coulomb system displays a bulk part that saturates quickly plus a surface contribution that varies on the scale of the linear dimensions of the system. We have chosen for this purpose a TCP with regularized interactions between unlike charges.

The potential is given by

$$V_{++}(|r|) = V_{--}(|r|) = -q^2 \ln(|r|/\sigma) \tag{4.3}$$

$$\begin{aligned} V_{+-}(|r|) &= q^2 \ln(|r|/\sigma); && |r| \geqslant \sigma \\ &= -\tfrac{1}{2}q^2 + \tfrac{1}{2}q^2(r/\sigma)^2; && |r| \leqslant \sigma \end{aligned} \tag{4.4}$$

The potential $V_{+-}(|r|)$ is the potential between a point charge and a charged disk. The radius σ of the disk used as the scale length of the Coulomb potential is chosen to be 1/10 of the ionic radius a defined by $\pi a^2 = \rho_b^{-1}$.

Because the interactions are completely symmetric, the truncated pair correlation function is equivalent to one-half the charge–charge correlation function, which is easily obtained in a computer simulation. The partial second moment displayed in Fig. 8, although very noisy, looks very similar to the one obtained on the OCP. While noisy, this curve is a convincing demonstration that there is a long-ranged "surface" contribution to the susceptibility.

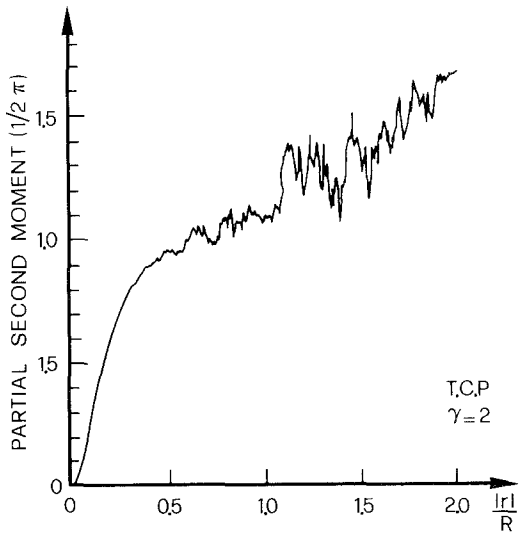

Fig. 8. Partial second moment of a TCP for $\gamma = 2$ and 2×50 particles. The noise in the charge–charge correlation function is strongly amplified by the factor $|r|^2$ in the integrand of the SM. Yet, the "arc sine" law is clearly visible.

5. ANISOTROPIC GEOMETRY

We study in this section the effect of a noncircular shape on the mean square fluctuations of the polarization of a system in the plasma state. Monte Carlo simulations for an OCP and also a TCP at high temperature, typically $\gamma = 2$, are compared to the result given by electrostatics. The shape of the simulation cells is chosen as an ellipse, since we can explicitly compute the components of the susceptibility tensor.

We first compute the potential produced by a uniformly charged background lying on a ellipse, which we need for the MC simulations of the OCP. In a second step, we derive from this potential the depolarization tensor and the susceptibility tensor defined by Eq. (2.16).

The potential of a homogeneously charged background of charge density 1 is given by

$$V_b = \int_A d^2y\, C(x, y) \tag{5.1}$$

where $C(x, y) = -\ln |x - y|$.

Following the procedure given in Ref. 11, p. 1202, we replace x by the complex variable $z = x_1 + ix_2$ and use the conformal mapping

$$z = \tfrac{1}{2}a \operatorname{ch} w; \qquad w = \mu + i\varphi \tag{5.2}$$

The variables μ and φ are the elliptic coordinates describing an ellipse with focus at $+a/2$ and $-a/2$, with major axis achk and minor axis ashk.

The kernel $C(z, z')$ is rewritten in the coordinates μ, φ and ν, ψ and expanded in a Taylor series [Ref. 11, Eq. (10.1.32)]

$$\begin{aligned} C(\mu, \varphi; \nu, \psi) = &-\left(\nu + \ln \frac{a}{4}\right) \\ &+ \sum_{n=1}^{\infty} \frac{2}{n} [\operatorname{ch} n\mu \cos n\varphi \exp(-n\nu) \cos n\psi \\ &+ \operatorname{sh} n\mu \sin n\varphi \exp(-n\nu) \sin n\psi] \end{aligned} \tag{5.3}$$

for $\mu < \nu$ and conversely for $\nu < \mu$.

The volume element $d^2y = \frac{1}{2}i\, dz'\, dz'^*$ becomes

$$\begin{aligned} \frac{i}{2} \frac{dz'}{dw'} \frac{dz'^*}{dw'^*} dw'\, dw'^* &= \frac{i}{2} \frac{a^2}{4} \operatorname{sh} w' \operatorname{sh} w'^*\, dw'\, dw'^* \\ &= \frac{a^2}{8} (\operatorname{ch} 2\nu - \cos 2\psi)\, d\nu\, d\psi \end{aligned} \tag{5.4}$$

After integration over ψ and v $(0 \leqslant \mu \leqslant k)$ we obtain the simple result

$$V_b(\mu, \varphi) = -\tfrac{1}{16}\pi a^2(\operatorname{ch} 2\mu + \cos 2\varphi) + \tfrac{1}{16}\pi a^2 \operatorname{ch} 2\mu \cos 2\varphi \, e^{-2k} + \text{const} \quad (5.5)$$

Since we suspect that the result is of the form

$$V_b(x) = -b_1 x_1^2 - b_2 x_2^2 \quad (5.6)$$

with $x_1 + ix_2 = z$, we introduce in Eq. (5.5) the coordinates μ, φ and determine the constant b_1 and b_2 by comparison. We obtain

$$b_1 = \tfrac{1}{2}\pi(1 - e^{-2k}) \quad (5.7)$$

$$b_2 = \tfrac{1}{2}\pi(1 + e^{-2k}) \quad (5.8)$$

To check the result, we verify that

$$-\Delta V_b = 2(b_1 + b_2) = 2\pi$$

In order to express the potential in terms of the dimensions L_1 and L_2, which are the length and the width of the ellipse, we use the relations $L_1 = a \operatorname{ch} k$ and $L_2 = a \operatorname{sh} k$ and find

$$b_1 = \pi L_2/(L_1 + L_2); \qquad b_2 = \pi L_1/(L_1 + L_2) \quad (5.9)$$

We now use this result to compute the depolarization tensor given by Eq. (2.8):

$$T_A^{ij} = -\frac{1}{2\pi} \frac{\partial^2}{\partial x_i \, \partial x_j} V_b(x) = \frac{1}{\pi} b_i \delta_{ij} \quad (5.10)$$

and we obtain the components of the susceptibility tensor given by Eq. (2.16),

$$\chi_{11} = \frac{1}{2\pi} \frac{L_1 + L_2}{L_2}; \qquad \chi_{22} = \frac{1}{2\pi} \frac{L_1 + L_2}{L_1} \quad (5.11)$$

Note that the ratio of the longitudinal to the transverse susceptibilities is given by

$$\chi_{11}/\chi_{22} = L_1/L_2 \quad (5.12)$$

This relation has been examined with an OCP for $\gamma = 8$ (intermediate temperature with few collisions with the wall) for a system of 100 particles. The results are averaged on 600,000 moves per particle. This large number of configurations is necessary in order to obtain reasonably good results. The results are reported in Table I.

Table I. The OCP for $\gamma = 8$ and 600,000 Moves per Particle[a]

L_2/L_1	χ_{11}	χ_{11}^{th}	χ_{22}	χ_{22}^{th}	χ_{22}/χ_{11}	$\chi_{22}^{th}/\chi_{11}^{th}$
1	0.98	1.0	0.98	1.00	1.00	1.0
2	0.74	0.75	1.47	1.50	2.00	2.0
3	0.65	0.66	1.96	2.00	3.01	3.0

[a] χ_{11} and χ_{22} are the susceptibilities obtained by MC simulation, and χ_{11}^{th} and χ_{22}^{th} are the predictions of electrostatics in units of $1/\pi$.

Table II. The TCP for $\gamma = 1.0$ and 300,000 Moves per Particle[a]

L_2/L_1	χ_{11}	χ_{11}^{th}	χ_{22}	χ_{22}^{th}	χ_{22}/χ_{11}	$\chi_{22}^{th}/\chi_{11}^{th}$
1	0.84	1.0	0.842	1.0	1.00	1.00
2	0.60	0.75	1.29	1.5	2.15	2.00
3	0.523	0.66	1.75	2.0	3.34	3.0

[a] χ_{11} and χ_{22} are the susceptibilities obtained by MC simulation, and χ_{11}^{th} and χ_{22}^{th} are the predictions of electrostatics in units of $1/\pi$.

Table II shows the results for a TCP with twice 50 particles and with the regularized interaction [Eq. (4.4)]. The size of the parabolic core radius is one-tenth the mean ionic radius. We have obtained the results by averaging over 300,000 moves per particle. While some information about the shape of the system was explicitly contained in the Hamiltonian of the OCP, this system does not have any knowledge of the elliptic form besides that provided by the collisions of its particles with the wall.

One can see from the tables that the susceptibilities of both the OCP and the TCP are all below the theoretical predictions. It is known already from simulations reported in I that the susceptibility has a strong size and N dependence, and we would have needed many more particles in order to avoid the saturation effect due to the finite size of the system. However, the ratio for the susceptibilities is in good agreement with the predictions of electrostatics.

6. THE OCP ON A STRIP FOR $\gamma = 2$

We consider here the strip geometry. The system is placed between a pair of infinite straight lines separated from each other by a width $2L$. We

call the directions parallel and perpendicular to the lines transverse and longitudinal, respectively. Furthermore, we assume that the lines bear no surface charge and that the system is surrounded by vacuum.

Due to the anisotropy of the dielectric susceptibility tensor in this geometry we have to distinguish here the longitudinal component χ_L from the transverse one(s) χ_T.

According to Eq. (2.11), the relations between the dielectric constant and the longitudinal component χ_L and the transverse component(s) χ_T are

$$\varepsilon^{-1} = 1 - (\nu - 1)\, 2\pi\chi_L; \qquad \nu = 2, 3 \tag{6.1}$$

$$\varepsilon = 1 + (\nu - 1)\, 2\pi\chi_T; \qquad \nu = 2, 3 \tag{6.2}$$

It follows from these two relations and from Eq. (2.16) that the values of the susceptibility in the plasma state are respectively given by

$$\chi_L = 1/[(\nu - 1)\, 2\pi]; \qquad \nu = 2, 3 \tag{6.3}$$

$$\chi_T = \infty \tag{6.4}$$

For the transverse susceptibility, the consistency between classical electrostatics and statistical mechanics is demonstrated by the results of Forrester and Smith[12] for the truncated two-particle correlation function of the 2D OCP for $\gamma = 2$ in a strip geometry. Indeed, the latter have shown that an asymptotic expansion of the two-particle correlation function for two particles located at $(x_1, 0)$ and (x_2, y) for large y (y being the pair separation in the transverse direction) displays the polynomial decay first described by Jancovici[13] in the case of a half-space, namely as $-y^{-2}$ when y tends to infinity. Therefore, it is obvious that the SM formula diverges in the thermodynamic limit.

In the longitudinal case, it has been proved[12] that the one- and two-particle correlation functions can be given explicitly for the 2D OCP for $\gamma = 2$. We recall that the result has been obtained by first considering an annulus of width $2L$ with inner and outer radii $R - L$ and $R + L$, respectively. In the limit $R \to \infty$ with L fixed, the boundary becomes a pair of straight lines separated by a region of width $2L$. Assuming the surface charge of the straight lines is zero, one can write the one-particle correlation function given in Ref. 12,

$$\rho_1(x) = \rho h(x) \tag{6.5}$$

where

$$h(x) = \frac{2}{\sqrt{\pi}} \int_0^Y dt\, \frac{\exp[-(t + Y - Kx)^2] + \exp[-(t - Y + Kx)^2]}{\operatorname{erf}(t + Y) - \operatorname{erf}(t - Y)} \tag{6.6}$$

ρ_b is the charge density of the background, $K=(2\pi\rho_b)^{1/2}$, $Y=KL$ is a dimensionless parameter, and erf(s) is the error function defined by

$$\mathrm{erf}(s)=\frac{2}{\sqrt{\pi}}\int_0^s dx\,\exp(-x^2) \tag{6.7}$$

The two-particle correlation function for two particles sitting at $(x_1, 0)$ and (x_2, y) may be written in the form

$$\rho_2(x_1, x_2, y)=\rho_b^2\{h(x_1)\,h(x_2)-\exp(-\pi\rho_b r_{12}^2)\,|h(\tfrac{1}{2}(x_1+x_2+iy))|^2\} \tag{6.8}$$

where

$$r_{12}^2=(x_1-x_2)^2+y^2 \tag{6.9}$$

For convenience, we set

$$D(t, Y)=\mathrm{erf}(t+Y)-\mathrm{erf}(t-Y) \tag{6.10}$$

and

$$G=(x_1+x_2)/2 \tag{6.11}$$

Using Eq. (6.5), Eq. (2.26) becomes

$$\chi_{\mathrm{L}}=\frac{\rho_b}{L}\int_0^{2L} dx\,x^2h(x)+\frac{1}{L}\int_0^{2L} dx_1\,x_1\int_0^{2L} dx_2\,x_2\int_{-\infty}^{+\infty} dy\,\rho_2^T(x_1, x_2, y) \tag{6.12}$$

We call χ_{L}^1 the first term on the rhs of Eq. (6.12) and χ_{L}^2 the second term.

Using Eqs. (6.6) and (6.10), χ_{L}^1 becomes

$$\chi_{\mathrm{L}}^1=\frac{2}{\sqrt{\pi}}\frac{\rho_b}{L}\int_0^Y\frac{dt}{D(t, Y)}\int_0^{2L} dx\,x^2 \times\{\exp[-(t+Y-Kx)^2]+\exp[-(t-Y+Kx)^2]\} \tag{6.13}$$

which can also be written, using suitable changes of variables,

$$\chi_{\mathrm{L}}^1=\frac{2}{\pi^{3/2}}\frac{1}{KL}\int_0^Y\frac{dt}{D(t, Y)}\int_{t-Y}^{t+Y} du\,[Y^2+(t-u)^2]\exp(-u^2) \tag{6.14}$$

The above expression can be calculated directly. We find

$$\chi_L^1 = \frac{1}{2\pi}\left(1+\frac{8(KL)^2}{3}\right) - \frac{1}{\pi^{3/2}}\frac{1}{KL}\left(\int_0^Y \frac{dt}{D(t,Y)}\{(t+Y)\exp[-(t+Y)^2] - (t-Y)\exp[-(t-Y)^2]\} - 2\int_0^Y \frac{dt}{D(t,Y)} t\{\exp[-(t+Y)^2]-\exp[-(t-Y)^2]\}\right) \quad (6.15)$$

For χ_L^2 the result is (cf. Appendix)

$$\chi_L^2 = -\frac{1}{2\pi}\frac{8(KL)^2}{3} - \frac{2}{\pi^{3/2}}\frac{1}{KL}\int_0^Y \frac{dt}{D(t,Y)} t\{\exp[-(t+Y)^2]-\exp[-(t-Y)^2]\} - \frac{1}{\pi^2}\frac{1}{KL}\int_0^Y \frac{dt}{D^2(t,Y)}\{\exp[-(t+Y)^2]-\exp[-(t-Y)^2]\}^2 \quad (6.16)$$

Gathering Eqs. (6.15) and (6.16), we obtain

$$\chi_L = \chi_L^1 + \chi_L^2 = \frac{1}{2\pi} - \frac{C(Y)}{2KL} \quad (6.17)$$

where

$$C(Y) = 2\left(\frac{1}{\pi^{3/2}}\int_0^Y \frac{dt}{D(t,Y)}\{(t+Y)\exp[-(t+Y)^2] - (t-Y)\exp[-(t-Y)^2]\} + \frac{1}{\pi^2}\int_0^Y \frac{dt}{D^2(t,Y)}\{\exp[-(t+Y)^2]-\exp[-(t-Y)^2]\}^2\right) \quad (6.18)$$

It is possible to find a simple expression for $C(Y)$ by noting the following relations. From the definition [Eq. (6.10)] of $D(t, Y)$ we have

$$\frac{\partial D(t,Y)}{\partial t} = \frac{2}{\sqrt{\pi}}\{\exp[-(t+Y)^2]-\exp[-(t-Y)^2]\} \quad (6.19)$$

$$\frac{\partial^2 D(t,Y)}{\partial t^2} = -\frac{4}{\sqrt{\pi}}\{(t+Y)\exp[-(t+Y)^2]-(t-Y)\exp[-(t-Y)^2]\} \quad (6.20)$$

Thus

$$C(Y)=2\left[-\frac{1}{4\pi}\int_0^Y \frac{dt}{D(t,Y)}\frac{\partial^2 D(t,Y)}{\partial t^2}+\frac{1}{4\pi}\int_0^Y \frac{dt}{D^2(t,Y)}\left(\frac{\partial D(t,Y)}{\partial t}\right)^2\right]$$

$$=2\left[-\frac{1}{4\pi}\frac{1}{D(t,Y)}\frac{\partial D(t,Y)}{\partial t}\bigg|_0^Y\right.$$

$$\left.-\frac{1}{4\pi}\int_0^Y \frac{dt}{D^2(t,Y)}\left(\frac{\partial D(t,Y)}{\partial t}\right)^2+\frac{1}{4\pi}\int_0^Y \frac{dt}{D^2(t,Y)}\left(\frac{\partial D(t,Y)}{\partial t}\right)^2\right]$$

$$=\frac{1}{\pi^{3/2}}\frac{1-\exp(-4Y^2)}{\operatorname{erf}(2Y)} \tag{6.21}$$

As $Y\to\infty$ we find $C(\infty)=\pi^{-3/2}$ instead of the value given in I and $\chi_L=1/2\pi$, which is the result given by Eq. (6.3) for $\nu=2$.

7. THE 2D OCP ON A SPHERE FOR $\gamma=2$

We consider now the case of N identical particles of charge q confined at the surface of a sphere centered in O and of radius R. The interest in such a geometry resides in the fact that this system has no boundary and therefore that the value predicted by the SL sum rule should be recovered. This is effectively what happens, as we now prove.

For such a system and for $\gamma=2$, it has been shown[14] that the n-particle correlation functions $\rho_N^{(n)}(1,2,\ldots,n)$ can be given explicitly. In particular, the one- and two-particle correlation functions are given by

$$\rho_N^{(1)}(1)=\rho \tag{7.1}$$

$$\rho_N^{(2)}(1,2)=\rho^2 g_N^{(2)}(1,2) \tag{7.2}$$

where

$$\rho=N/4\pi R^2 \tag{7.3}$$

is the number density, where

$$g_N^{(2)}(1,2)=1-\left(\frac{1+\cos\psi_{12}}{2}\right)^{N-1} \tag{7.4}$$

and

$$\psi_{ij}=\arccos\frac{OR_i\cdot OR_j}{R^2} \tag{7.5}$$

is the angle between the two vectors pointing to the particles i and j located on the surface of the sphere.

Since Eq. (7.4) is rotational invariant, we can use the SM formula to compute the susceptibility.

Choosing as polar axis for the second sphere the OR_1 direction and designating by (ψ, ϕ) its spherical coordinates, we have for Eq. (2.27) the convenient form

$$\chi^{\text{sphere}} = \frac{4\pi\rho^2 R^6}{|\Lambda|} \int_0^{2\pi} d\phi \cos^2\phi \int_0^{\pi} d\psi \left(\frac{1+\cos\psi}{2}\right)^{N-1} \sin^3\psi \tag{7.6}$$

where the factor 4π comes from the integration over the solid angle of the first sphere $d\Omega_1 = \sin\theta_1\, d\theta_1\, d\varphi_1$ and where $|\Lambda| = 4\pi R^2$.

The integration can be performed easily. One obtains

$$\begin{aligned}\chi^{\text{sphere}} &= \frac{8\pi^2}{2^N} \frac{\rho^2 R^6}{4\pi R^2} \int_{-1}^{+1} dx\,(1-x^2)(1+x)^{N-1} \\ &= \frac{1}{2\pi} \frac{N^2}{(N+1)(N+2)}\end{aligned} \tag{7.7}$$

The asymptotic expansion of Eq. (7.7) yields

$$\chi^{\text{sphere}} = \frac{1}{2\pi}\left[1 - \frac{3}{N} + O(N^{-2})\right] \tag{7.8}$$

We observe that the electrostatic value is reached with a first-order correction proportional to the reciprocal of the area of the sphere, i.e., more rapidly than in the case of the disk, where the correction is $O(R^{-1})$, or of the strip, where it is $O(L^{-1})$. To give a numerical example, for the susceptibility to have 97% of its infinite-system value, we need 694 particles on a disk, but only 100 particles on a sphere.

In the thermodynamic limit, Eq. (7.7) becomes

$$\lim_{N\to\infty} \chi^{\text{sphere}} = 1/(2\pi) \tag{7.9}$$

which is the value given by the SL sum rule.

APPENDIX. CALCULATION OF χ_L^2

By definition,

$$\chi_L^2 = \frac{1}{L} \int_0^{2L} dx_1\, x_1 \int_0^{2L} x_2\, dx_2 \int_{-\infty}^{+\infty} dy\, \rho_2^T(x_1, x_2, y)$$

We first integrate over y. The explicit expression for $\rho_2^T(x_1, x_2, y)$ can be easily obtained using its definition and Eqs. (6.5), (6.8), (6.9), and (6.11).

We find

$$\rho_2^T(x_1, x_2, y) = \rho_2(x_1, x_2, y) - \rho_1(x_1)\,\rho_1(x_2)$$
$$= -\rho_b^2 \exp\{-\pi\rho_b[(x_1-x_2)^2+y^2]\} \cdot |h(G+\tfrac{1}{2}iy)|^2 \qquad \text{(A.1)}$$

Further, using Eq. (6.6), we obtain for the integral over y

$$\int_{-\infty}^{+\infty} dy\, \rho_2^T(x_1, x_2, y)$$
$$= -\frac{4\rho_b^2}{\pi}\left(\int_{-\infty}^{+\infty} dy \exp\{-\pi\rho_b[(x_1-x_2)^2+y^2]\}\right.$$
$$\left.\times \int_0^Y \frac{ds\,dt}{D(s)\,D(t)}(AC+AD+BC+BD)\right) \qquad \text{(A.2)}$$

where

$$A = \exp[-(t+Y-KG-\tfrac{1}{2}Kiy)^2]$$
$$B = \exp[-(t-Y+KG+\tfrac{1}{2}Kiy)^2]$$
$$C = \exp[-(s+Y-KG+\tfrac{1}{2}Kiy)^2]$$
$$D = \exp[-(s-Y+KG-\tfrac{1}{2}Kiy)^2]$$

We shall call, respectively, T_1, T_2, T_3, and T_4 the four terms on the rhs of Eq. (A.2). Since the calculations are analogous for the four terms, we present here the calculation for T_1 only.

Noticing that the product AC can be written as

$$AC = \exp(-\alpha^2-\beta^2)\exp[iK(t-s)\,y+\tfrac{1}{2}K^2y^2]$$

with $\alpha = t+Y-KG$ and $\beta = s+Y-KG$, we see that T_1 becomes, after permutation of the integrals over y with the integrals over s and t,

$$T_1 = -\frac{4\rho_b^2}{\pi}\exp[-\pi\rho_b(x_1-x_2)^2]\int_0^Y \frac{ds\,dt}{D(s)\,D(t)}\exp(-\alpha^2-\beta^2)$$
$$\times\int_{-\infty}^{+\infty} dy \exp\left[-\pi\rho_b y^2 + iK(t-s)\,y+\frac{1}{2}K^2y^2\right]$$

The integral over y can be simplified and we have

$$\int_{-\infty}^{+\infty} dy \exp\left[-\pi\rho_b y^2 + iK(t-s)\,y+\frac{1}{2}K^2y^2\right]$$
$$= \int_{-\infty}^{+\infty} dy \exp[iK(t-s)\,y] = 2\pi\delta[K(t-s)]$$

where δ is the Dirac delta function.

Finally, using the property of the delta function that $\delta(Kx) = \delta(x)/K$, we obtain the following result:

$$T_1 = -\frac{8\rho_b^2}{K} \exp[-\pi\rho_b(x_1 - x_2)^2] \int_0^Y \frac{dt}{D^2(t)} \exp[-2(t + Y - KG)^2] \quad \text{(A.3)}$$

In the same way, we show that

$$T_4 = -\frac{8\rho_b^2}{K} \exp[-\pi\rho_b(x_1 - x_2)^2] \int_0^Y \frac{dt}{D^2(t)} \exp[-2(t - Y + KG)^2] \quad \text{(A.4)}$$

whereas

$$T_2 = T_3 = 0 \quad \text{(A.5)}$$

The fact that T_2 and T_3 vanish results from the appearance in these two expressions of a term in $\delta(t+s)$ and not $\delta(t-s)$ as before. Now, because $s \in [0, Y]$ and $t \in [0, Y]$ with $Y > 0$, we see tat the effect of $\delta(t+s)$ is to cancel the integration over s and t.

Then it follows from Eqs. (A.3)–(A.5) that the integral over y of the truncated two-point distribution function is given by

$$\begin{aligned} &\int_{-\infty}^{+\infty} dy\, \rho_2^T(x_1, x_2, y) \\ &\quad = -\frac{8\rho_b^2}{K} \left\{ \int_0^Y \frac{dt}{D^2(t)} \exp[-\pi\rho_b(x_1 - x_2)^2 - 2(t + Y - KG)^2] \right. \\ &\qquad \left. + \int_0^Y \frac{dt}{D^2(t)} \exp[-\pi\rho_b(x_1 - x_2)^2 - 2(t - Y + KG)^2] \right\} \end{aligned} \quad \text{(A.6)}$$

Thus, using Eq. (A.6), one can write χ_L^2 as

$$\begin{aligned} \chi_L^2 = \frac{-8\rho_b^2}{KL} \Bigg(&\int_0^Y \frac{dt}{D^2(t)} \exp[-2(t + Y)^2] \\ &\times \left\{ \int_0^{2L} dx\, x \exp[-K^2x^2 + 2K(t + Y)\, x] \right\}^2 \\ &+ \int_0^Y \frac{dt}{D^2(t)} \exp[-2(t - Y)^2] \\ &\times \left\{ \int_0^{2L} dx\, x \exp[-K^2x^2 - 2K(t - Y)\, x] \right\}^2 \Bigg) \end{aligned} \quad \text{(A.7)}$$

The two integrals over x can be easily calculated using suitable changes of variables, Eqs. (6.7) and (6.10). Then Eq. (A.7) becomes

$$\chi_L^2 = -\frac{1}{2\pi}\frac{8(KL)^2}{3} - \frac{2}{\pi^{3/2}}\frac{1}{KL}\int_0^Y \frac{dt}{D(t)}\, t\{\exp[-(t+Y)^2] - \exp[-(t-Y)^2]\} - \frac{1}{\pi^2}\frac{1}{KL}\int_0^Y \frac{dt}{D^2(t)}\{\exp[-(t+Y)^2] - \exp[-(t-Y)^2]\}^2 \quad \text{(A.8)}$$

ACKNOWLEDGMENTS

We thank E. R. Smith for his help in preparing the manuscript, and G. Doolen, B. Jancovici, and Ph. A. Martin for their stimulating interest in this work. Financial support from the Center for Materials Study of the Los Alamos National Laboratories and from the Swiss National Funds is gratefully acknowledged.

REFERENCES

1. C. Kittel, *Introduction to Solid State Physics*, 4th ed. (Wiley, New York, 1971), Chapter 13.
2. J. D. Jackson, *Classical Electrodynamics*, 2nd ed. (Wiley, New York, 1975), Sections 4.3–4.5.
3. *Handbuch der Physik*: *Dielektrika*, Band XVII (Springer-Verlag, 1956), Sections 22–24.
4. O. F. Mossotti, *Memorie di Matematica e di Fisica della Società Italiana delle Scienze residente in Modena* **XXIV**(2):49–74 (1850).
5. R. Clausius, *Die mechanische Wärmetheorie*, 2nd ed. (Friedrich Vieweg, Braunschweig, 1879), Vol. 2, pp. 62–97.
6. R. Becker, *Electromagnetic Fields and Interactions* (Blaisdell, 1964), pp. 102–107.
7. S. R. De Groot and L. G. Suttorp, *Foundations of Electrodynamics* (North-Holland, Amsterdam, 1972), pp. 106–109.
8. J. A. Osborn, *Phys. Rev.* **67**:351 (1945).
9. E. C. Stoner, *Phil. Mag.* **36**:803 (1945).
10. E. R. Smith and P. Wielopolski, *J. Phys. A*: *Math. Gen.* **15**:2557–2568 (1982).
11. P. M. Morse and H. Feshbach, *Methods of Theoretical Physics*, Part 2, (McGraw-Hill, New York, 1953).
12. P. J. Forrester and E. R. Smith, *J. Phys. A*: *Math. Gen.* **15**:3861–3868 (1982).
13. B. Jancovici, *J. Stat. Phys.* **28**:43 (1982).
14. J. M. Caillol, *J. Phys. Lett.* **42**:L-245–247 (1981).
15. Ph. Choquard, B. Piller, and R. Rentsch, *J. Stat. Phys.* **43**:197 (1986).